Three-dimensional time-dependent MHD simulation model of the solar corona and solar wind

K. Hayashi

W. W. Hansen Experimental Physics Laboratory, Stanford University, USA

Abstract. We will present the MHD simulation model for the solar corona and solar wind. The simulation utilizes the solar photospheric magnetic field measurement data as the boundary condition, and the obtained MHD solution is fully matching the given solar surface magnetic field distribution. In order that the simulated situation will be more realistic, the boundary treatment in our code is based on the concept of the projected normal characteristic method, so that the boundary conditions other than magnetic field can be imposed without inconsistencies in physics and mathematics. The obtained three-dimensional MHD structure of the solar corona and solar wind can be tested by comparing with the in-situ measurement data. This simulation approach will provide us keys to better understandings about the dynamics of the solar coronal structures such as streamers and corona holes.

Index Terms. MHD simulation, solar corona, solar photospheric magnetic field, solar wind.

1. Introduction

The time-dependent multi-dimensional magneto-hydro-dynamic (MHD) simulation is today one of the major methods to determine the structures of the solar corona and solar wind, because it is generally very difficult to analytically calculate the solution of the nonlinear MHD equations. The MHD simulations are essential tools for the studies of the solar wind and solar corona as well as for the space weather prediction studies.

For example, when the global multi-dimensional structure of the solar corona and solar wind at a specified period were to be determined, only the time-relaxation method with the time-dependent MHD simulation can determine the solutions. Note that generally it is very difficult to determine the values of the plasma and magnetic field from the observations, because the solar corona and solar wind is optically thin for most wavelength ranges.

In addition, the time-dependent MHD simulation can simulate the responses of the solar wind and solar corona to the solar eruptive events such as flare and coronal mass ejection (CME). In this case, the model to initiate or mimic the CME events is needed, and the MHD simulation model can be coupled with these models.

In this paper, we will briefly show some of our efforts on the MHD simulations of the solar wind and solar corona: The basic features of the MHD simulation code and model, the results of the time-relaxation simulation for the solar corona, and the MHD simulation of the interplanetary disturbances.

2. MHD simulation model

The details of the MHD simulation code we have developed is described (Hayashi, 2005). The governing equations are the MHD equations written in the frame rotating with the Sun;

$$\frac{\partial \rho}{\partial t} = -\nabla \cdot (\rho \mathbf{v})$$

$$\frac{\partial (\rho \mathbf{v})}{\partial t} = -\nabla (P + \rho \mathbf{v}:\mathbf{v}) + \frac{1}{4\pi}\nabla \left[\mathbf{B}:\mathbf{B} - \frac{1}{2}B^2 \mathbf{I} \right] + \rho \left(\mathbf{g} + (\boldsymbol{\Omega}\times\mathbf{r})\times\boldsymbol{\Omega} + 2\mathbf{v}\times\boldsymbol{\Omega} \right)$$

$$\frac{\partial \mathbf{B}}{\partial t} = -\nabla \cdot \left(\mathbf{v}:\mathbf{B} - \mathbf{B}:\mathbf{v} \right)$$

$$\frac{\partial}{\partial t}\left[\frac{1}{2}\rho \mathbf{v}^2 + \frac{P}{\gamma - 1} + \frac{1}{8\pi}B^2 \right] = -\nabla \cdot \left[\left(\frac{1}{2}\rho \mathbf{v}^2 + \frac{\gamma P}{\gamma - 1} \right) \cdot \mathbf{v} - \frac{1}{4\pi}(\mathbf{v}\times\mathbf{B})\times\mathbf{B} \right] + \rho \mathbf{v} \cdot \left[\mathbf{g} + (\boldsymbol{\Omega}\times\mathbf{r})\times\boldsymbol{\Omega} \right]$$

We chose the spherical coordinate system originating at the center of the Sun, so that we can specify the inner boundary condition from the measurement data such as magnetic field. The computational region is limited by the two (inner and outer) spheres. In case the simulation region contains the region distant from the Sun, the angular velocity of the solar rotation is set to zero and the inner boundary map is rotated so that large entrainment velocity at the distant region will be avoided.

The MHD equation set in the conservation form is solved with the total variant diminishing (TVD) method with a Godunov-type Riemann solver. The monotonic upstream scheme for conservation laws (MUSCL) is used to achieve

the spatial accuracy of third order. With TVD and MUSCL methods, the numerical error will be reasonably reduced. The finite volume method (FVM) is also employed to deal with the non-Cartesian coordinate system.

One of the difficulties in the MHD simulation for the solar corona is that the simulation models have to deal with the solar surface or the base of corona. This physical sub-Alfvenic boundary is set not only to limit the simulation region but to give the physical constraints from observational data. The number of constraints we can give is determined by the number of the incoming (outward from the Sun) magneto-acoustic waves and outgoing (inward to the Sun). While the total number of the MHD waves is 8, the number of incoming waves is 5 in almost all cases. Therefore, it is usually allowed to give five constraints. In addition, the relationship among the five constraints should satisfy the characteristic equations of the MHD hyperbolic system.

To deal with the computational difficulties on the sub-Alfvenic boundary, we employed the projected normal characteristic method (Wu and Wang, 1987). In case we fix the radial component of magnetic field on the inner boundary (solar surface), this method allows us to give two other constraints. As one of the two constraints, we chose to limit the mass flux escaping through the solar surface. This choice makes the total simulated solar wind close to the Ulysses' in-situ measurement. Therefore, this choice is also measurement-based. As the last constraint, we can have various choices such as fixed density, temperature and so on. These choices will produce good contrast of plasma parameters comparable to the observations.

With our simulation model with the TVD-MUSCL method and the projected normal characteristic method, the computational errors due to the presence of the sub-Alfvenic solar surface boundary will be significantly reduced. It must be mentioned here that many similar studies have been already done (e.g. Usmanov, 1993; Linker et al., 1990; Linker et al., 1999). In these studies, the source surface potential field model (Schatten et al., 1969) and the Parker solution (Parker, 1958) are used as the initial magnetic field and plasma flow, respectively. We followed this simulation setup.

Fig. 1 shows the field lines of the solar corona given as the initial value (top) and that of the obtained steady state (bottom); During the time-relaxation process of about 40 hours in real time scale, the plasma at the initial closed field region will be stagnant, and that in the initial open field will flow outward from the Sun. The outer parts of the initial closed field regions will be open to the interplanetary space due to the presence of the plasma flow. It is clearly seen that the field lines of the closed field regions are stretched outward due to the gas pressure inside and the solar wind flow outside.

Through such nonlinear MHD interaction process between magnetic field and plasma, the simulated trans-Alfvenic flow reached the steady state. The obtained steady state in this way fully satisfies the MHD equilibrium and is fully consistent with the given magnetic field map.

3. Structures of the obtained steady solar corona

With the MHD simulation, we can obtain the plasma parameters as well as the magnetic field in three-dimension. The top panel of Fig. 2 demonstrates the density contrast near the bottom of the solar corona (1.03 solar radii from the center of the Sun) obtained with the MHD simulation. The bottom panel is the synoptic map format of the solar corona observed with SOHO/EIT. Because of the flexibility of the projected normal characteristic method, we can impose one constraint on the surface variables. The simulated density map (top of Fig. 2) was obtained with the assumption to fix the surface temperature (thus, density on the solar surface is varied with time).

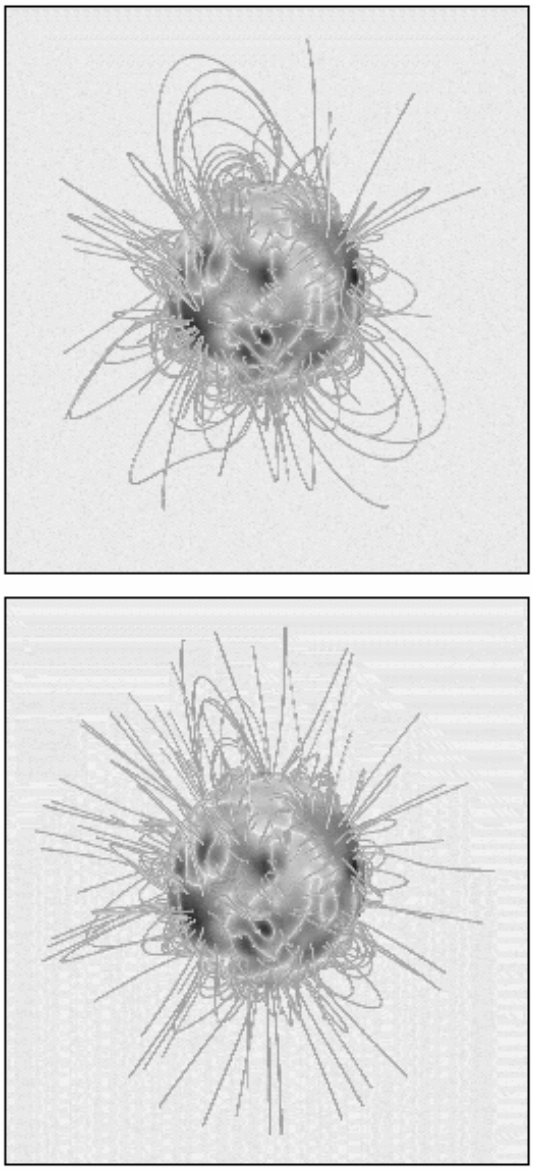

Fig. 1. Magnetic field lines in the solar corona; the initial potential field (top) and that of the steady state obtained with the time-relaxation simulation (bottom).

For this simulation, we give the initial potential field with the spherical harmonics polynomials up to fifth order, or the spatially averaged field map with the angular resolution of about 10 degrees. This simulation is done with a middle-scale simulation with the grid numbers of 72, 64 and 128 for radial, latitudinal and longitudinal directions, respectively.

A notable thing is that the dark (low-density) regions in the top panel well coincide with the observed coronal holes.

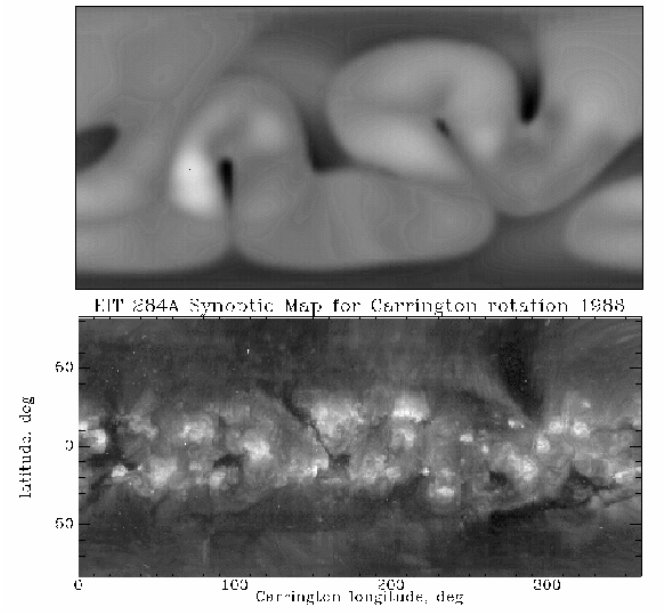

Fig. 2. The simulated density at the bottom of the solar corona (1.03 solar radii) and the synoptic format of the solar coronal brightness observed by the SOHO/EIT284A (bottom).

4. Solar wind at distant regions

In case the simulation region is only super-Alfvenic, the steady state of the solar wind can be obtained with the MHD simulation with the fixed conditions at the inner boundary. Fig. 3 shows the density on the solar equatorial plane obtained with the time-dependent MHD simulation for the region from 30 solar radii to 1350 solar radii (about 6.7 AUs). Considering the presence of the pick-up ion, we limited the simulation region, while we tested and confirmed that the simulation model can extend the simulation regions up to 20 to 30 AUs.

It should be emphasized that the radial increment method can also be used to obtain the steady MHD structure of the solar wind in the super-Alfvénic region. Because the radial increment method (e.g. Hayashi et al., 2003) needs less computer resources than the time-dependent simulation, it is very useful unless time-dependent phenomena such as interplanetary disturbance propagation are to be examined.

5. Simulation of interplanetary disturbances

A good test of the time-dependent MHD simulation of the solar wind is the simulation of the interplanetary disturbance propagation. This kind of simulation is quite useful for not only the space weather prediction but also the determination of the electromagnetic environment at the outer heliosphere.

As demonstrated in a work by Odstrcil et al. (2004), the parameters of the CME obtained from cone-model (Zhao et al., 2002) are very useful to determine the geometry and other information of CME, which are usually very difficult to determine. Probably, only the analysis of the interplanetary scintillation (IPS) of radio wave can do (e.g. Tokumaru, 2005). The CME parameters obtained can be used in the MHD simulation as the numerical perturbation to mimic the CME events and trace the temporal evolution of the driven interplanetary disturbances.

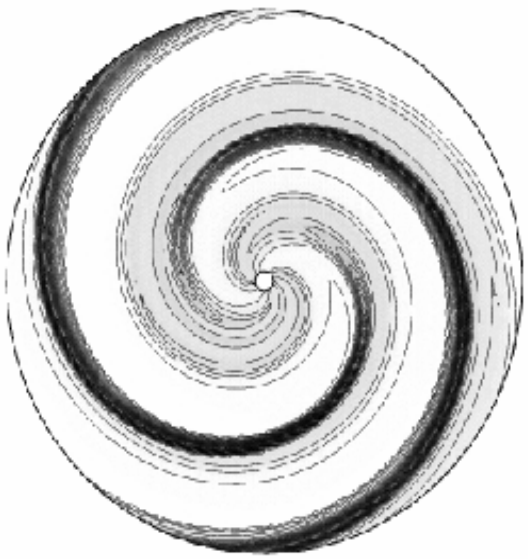

Fig. 3. The simulated density on the solar equatorial plane. The region shown is 30 solar radii (inner circle) to 6.7 AU (outer circle). The density is normalized with the square of the heliocentric distance. The evolution of the density at the trailing edge of the corotating interaction region (CIR) can be seen.

Fig. 4 demonstrates the temporal evolution of the density as the proxy of the interplanetary disturbances propagating in the co-rotating solar wind stream. In this simulation, the two numerical perturbations are given on the inner boundary, and the position, time of passage at 30 solar radii sphere (the inner simulation boundary), speed and spread angle of the two impulses are calculated from the cone-model analysis. We chose the period of April 2002, when two halo CME events occurred; the averaged speed of the first and second CME were estimated about 600 and 900 km/s, respectively.

Because of the different speeds, these two interplanetary disturbances merged at about 2 AU. These two disturbances were measured by nearby-Earth measurements, and the arrival times of these two simulated CME to the Earth agreed well with the measurements. Therefore, the estimation of the speed of CME with the cone-model must have been good, and it is reasonably expected that a collision of the two interplanetary disturbances actually occurred.

6. Summary

In this paper, we showed some examples of the MHD simulations of solar corona and solar wind; the MHD simulation of the trans-Alfvenic solar corona and solar wind, that of the super-Alfvenic solar wind, and the simulation of disturbance propagation utilizing the cone-model parameters.

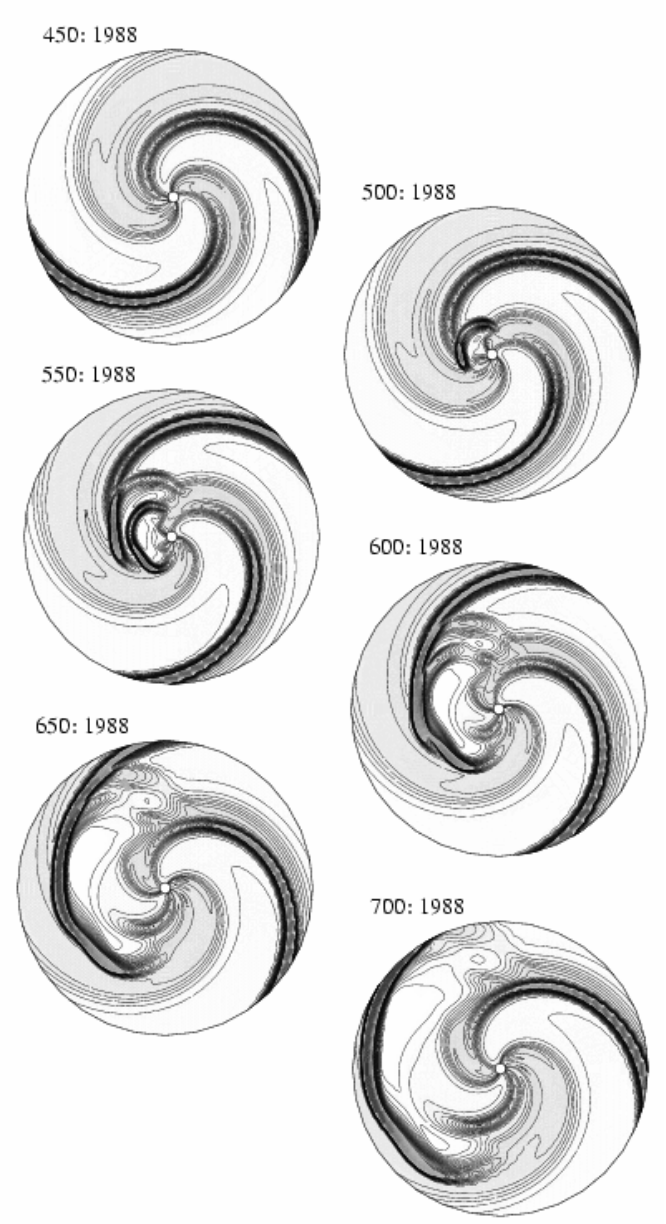

Fig. 4. The simulated interplanetary disturbance propagations on the solar equatorial plane within 750 solar radii (about 3.5 AUs). The two numerical perturbations parameterized with the Cone-Model are given on the inner boundary. In this simulated case, the collision occurred at about 2 AUs. The time interval of the plots is f 50 hours. The density is normalized with the square of the heliocentric distance.

The advantages of the MHD simulation are demonstrated; the nonlinear MHD equations are fully solved in the situation specified with the measurement/observation-based parameters, such as the magnetic field map and the interplanetary disturbance parameters. We would like to mention here that the MHD simulation can be flexible and include not only the measurement-based data but also some artificially modeled situations.

The author emphasizes that many simulation models of the solar wind and solar corona have been developed with various models for various scientific target objects. The optimal code should be made for each purpose, and our model is focused on obtaining the MHD solution of the trans-Alfvenic solar corona and solar wind with less inconsistency in physics and mathematics. However, the dynamics of the real solar corona and solar wind must be determined by the dynamics of the solar interior and the microscopic turbulent MHD phenomena such as magnetic reconnection and Alfven-wave decay, most of which our current model does not include for simplicity. Future modifications are necessary, and the MHD model shown in this paper can be the framework of the future comprehensive models of the solar wind and solar corona.

References

K. Hayashi, M. Kojima, M. Tokumaru and K. Fujiki, “MHD tomography using interplanetary scintillation measurement”, *J. Geophys. Res.*, vol 108, pp. 1102-1115, 2003.

K. Hayashi, “MHD Simulations of the Solar Corona and Solar Wind Using a Boundary Treatment to Limit Solar Wind Mass Flux” *Astrophys. J. Suppl. Series*, vol. 161, pp. 480-494, 2005.

J. A. Linker, G. van Hoven and D. D. Schnack, “A three-dimensional simulation of a coronal streamer”, *Geophys. Res. Lett.*, vol. 17, pp. 2281-2284, 1990.

J. A. Linker et al., “Magnetohydrodynamic modeling of the solar corona during whole Sun month”, *J. Geophys. Res.*, vol. 104, pp. 9809-9830, 1999.

D. Odstrcil, P. Riley and X. P. Zhao, “Numerical simulation of the 12 May 1997 interplanetary CME event”, *J. Geophys. Res.*, vol. 198, A02116, 2004.

E. N. Parker, “Dynamics of the interplanetary gas and magnetic fields” *Astrophys. J.*, vol. 128, pp. 664-676, 1958.

K. H. Schatten, J. M. Wilcox and N. F. Ness, “A model of interplanetary and coronal magnetic fields”, *Solar Phys*, vol. 6, p. 442, 1969.

M. Tokumaru, M. Kojima, K. Fujiki, M. Yamashita and D. Baba, “Interplanetary consequence caused by the extremely intense solar activity during October-November 2003”, *J. Geophys. Res.*, vol. 110, A01109, 2005.

A. V. Usmanov, “A global numerical 3-D MHD model of the solar wind”, *Solar Phys.*, vol. 146, p. 377, 1993.

S. T. Wu and J. F. Wang, “Numerical tests of a modified full implicit continuous Eulerian (FICE) scheme with projected normal characteristic boundary conditions for MHD flows”, *Computer Methods in Applied Mechanics and Engineering*, vol. 64, pp. 267-282, 1987.

X. P. Zhao, S. P. Plunkett and W. Liu, “Determination of geometrical and kinematical properties of halo coronal mass ejections using the cone model”, *J. Geophys. Res.*, vol. 108, pp. 1223-1231, 2002.